Published in final edited form as:
Nat Med. 2012 December ; 18(12): 1768–1777. doi:10.1038/nm.2979.

Obesity in mice with adipocyte-specific deletion of clock component *Arntl*

Georgios K Paschos[1], **Salam Ibrahim**[1], **Wen-Liang Song**[1], **Takeshige Kunieda**[1], **Gregory Grant**[1], **Teresa M Reyes**[1], **Christopher A Bradfield**[2], **Cheryl H Vaughan**[3], **Michael Eiden**[4], **Mojgan Masoodi**[4], **Julian L Griffin**[4], **Fenfen Wang**[5], **John A Lawson**[1], and **Garret A FitzGerald**[1]

[1]Perelman School of Medicine, Institute for Translational Medicine and Therapeutics, University of Pennsylvania, Philadelphia, Pennsylvania, USA.

[2]McArdle Laboratory, Department of Oncology, University of Wisconsin, School of Medicine and Public Health, Madison, Wisconsin, USA.

[3]Department of Biology, Center for Obesity Reversal, Georgia State University, Atlanta, Georgia, USA.

[4]Medical Research Council Human Nutrition Research, Elsie Widdowson Laboratory, Cambridge, UK.

[5]Perelman School of Medicine, Institute for Diabetes, Obesity and Metabolism, University of Pennsylvania, Philadelphia, Pennsylvania, USA.

Abstract

Adipocytes store excess energy in the form of triglycerides and signal the levels of stored energy to the brain. Here we show that adipocyte-specific deletion of *Arntl* (also known as *Bmal1*), a gene encoding a core molecular clock component, results in obesity in mice with a shift in the diurnal rhythm of food intake, a result that is not seen when the gene is disrupted in hepatocytes or pancreatic islets. Changes in the expression of hypothalamic neuropeptides that regulate appetite are consistent with feedback from the adipocyte to the central nervous system to time feeding behavior. Ablation of the adipocyte clock is associated with a reduced number of polyunsaturated fatty acids in adipocyte triglycerides. This difference between mutant and wild-type mice is reflected in the circulating concentrations of polyunsaturated fatty acids and nonesterified polyunsaturated fatty acids in hypothalamic neurons that regulate food intake. Thus, this study reveals a role for the adipocyte clock in the temporal organization of energy regulation, highlights timing as a modulator of the adipocyte-hypothalamic axis and shows the impact of timing of food intake on body weight.

Several components of energy homeostasis, including locomotor activity, feeding, thermogenesis, glucose and lipid metabolism, are subject to circadian regulation that

Correspondence should be addressed to G.A.F. (garret@upenn.edu).

AUTHOR CONTRIBUTIONS

G.K.P., S.I., W.-L.S., T.K., C.H.V. and F.W. contributed to the acquisition, analysis and interpretation of the data. G.K.P. and G.A.F. initiated and designed the study. G.G. performed statistical analyses and analysis of the microarray data. T.M.R. performed indirect calorimetric analyses. C.A.B. provided the mice with the conditional *Arntl* allele. M.E., M.M., J.L.G. and J.A.L. performed the liquid chromatography mass spectrometry (LC-MS) analysis. G.K.P. and G.A.F. wrote the paper.

COMPETING FINANCIAL INTERESTS

The authors declare no competing financial interests.

synchronizes energy intake, storage and utilization with changes in the external environment imposed by the rotation of the earth[1]. In mammals, the circadian clock of the hypothalamic suprachiasmatic nucleus (SCN) and clocks in peripheral tissues involved in energy homeostasis coordinate 24-h cycles in these aspects of physiology and behavior[2]. Animal models of global and discrete circadian clock dysfunction develop abnormalities in energy metabolism[3–7]. In humans, cross-sectional studies have uncovered an increased prevalence of obesity and metabolic syndrome in night-shift workers[8,9]. Patients with sleep disorders have a higher risk for developing obesity, and the duration of sleep is inversely correlated with body weight in healthy men and women[10].

The regulation of energy homeostasis requires integration of multiple signals between the central nervous system and the periphery. Adipose tissue participates in this system not only by storing and releasing energy but also by informing the central nervous system of the energy stored within it. White adipose tissue (WAT) secretes leptin to signal the levels of long-term stored energy to the central nervous system[11]. Leptin signaling in the central nervous system results in an increase in energy expenditure and a reduction of food intake by repression of orexigenic pathways and induction of anorexigenic pathways in the hypothalamus[12,13]. In addition, fatty acid release by WAT into the circulation is another mechanism by which WAT participates in the regulation of energy homeostasis. An increase in the concentration of circulating long-chain unsaturated fatty acids leads to a proportional increase in their concentration in the hypo-thalamus[14]. Hypothalamic neurons respond to increased intracellular concentrations of long-chain unsaturated fatty acids by inhibition of food intake[15,16].

Taken together, these lines of evidence are consistent with a central role for adipose tissue as an integrator of organismal energy balance through the regulation of both food intake and energy expenditure. What is not yet known is the physiological importance of the adipocyte circadian clock in the temporal organization of energy regulation.

RESULTS

Deletion of *Arntl* disrupts the adipocyte circadian clock

To study the role of the adipocyte circadian pacemaker in energy homeostasis, we generated mice lacking *Arntl* (also known as *Bmal1* or *Mop3*) in adipocytes[17]. Previous reports have shown that mice with deletion of *Arntl* in all tissues (*Arntl* knockout mice) have higher body weight[18] and greater adipose tissue mass[4] at 4–8 weeks of age compared to wild-type (WT) mice. Similarly to these reports, we found a trend toward greater adipose tissue mass in 8-week-old *Arntl* knockout mice compared to WT mice (Supplementary Fig. 1a). Starting at 14 weeks of age, the *Arntl* knockout mice developed progressive arthropathy followed by weight loss and features of accelerated aging[19], rendering the universal *Arntl* knockout mouse unsuitable for the study of energy homeostasis after this age. To generate adipocyte-specific deletion of *Arntl*, we bred mice with a conditional *Arntl* allele[20] (Fig. 1a) with mice expressing Cre recombinase under the control of the adipocyte-specific promoter of the adipocyte protein 2 (*aP2*) gene (*aP2*-Cre mice)[21]. To examine mice with *Arntl* deleted specifically in adipocytes (Ad-$Arntl^{-/-}$ mice) we used male C57BL/6J mice (Supplementary Fig. 1b) homozygous for the *Arntl* conditional allele carrying one copy of the Cre recombinase transgene together with littermate mice homozygous for the *Arntl* conditional allele but not carrying Cre recombinase (control mice). In the presence of Cre recombinase, 75% and 50% of *Arntl* was excised in primary adipocytes isolated from white epididymal fat and brown interscapular fat, respectively (Fig. 1b,c). Cre recombinase led to 82% and 74% lower expression of *Arntl* in white and brown adipocytes, respectively, of Ad-$Arntl^{-/-}$ mice relative to adipocytes from WT mice (Fig. 1d,e). Arntl protein was not detectable in either white or brown adipocytes of Ad-$Arntl^{-/-}$ mice (Fig. 1f,g). We tested other tissues from

these mice for loss of *Arntl* and found excision in peritoneal macrophages but not any other tissues examined (Fig. 1h). Excision of *Arntl* was evident in epididymal WAT and interscapular brown adipose tissue (BAT) from Ad-*Arntl*$^{-/-}$ mice (Fig. 1h). The amount of excision of *Arntl* in WAT was lower compared to the excision in isolated primary adipocytes in these mice as a result of existence of cells other than adipocytes in WAT. To control for the excision of *Arntl* in macrophages, we generated mice with *Arntl* deletion specifically in myeloid cells (M-*Arntl*$^{-/-}$ mice) using mice that express Cre recombinase under the control of the lysozyme M promoter (LysM-Cre)[22] (Supplementary Fig. 1c,d).

We next investigated whether the circadian clock is disrupted in white and brown adipocytes. Clock and clock-output genes show rhythmic expression in WAT and BAT from WT mice (Supplementary Fig. 1f,g); however, the rhythmic expression of clock and clock-output genes is abolished in WAT and BAT from *Arntl* knockout mice, indicating disruption of clock function (Supplementary Fig. 1f,g). Similarly to WT mice, the expression of the circadian clock genes *Arntl*, *Nr1d1* (also known as *Rev-erb*α) and *Per1*–3 and the clock-output genes *Dbp* and *Nfil3* (also known as *E4bp4*) oscillates across time in both WAT and BAT from control mice kept under constant darkness (Fig. 1i,j). This indicates the existence of a functional circadian clock in mice carrying the conditional *Arntl* allele in both white and brown adipocytes and confirms our previous findings indicating that the conditional *Arntl* allele functions in the same way as a WT allele[20]. In Ad-*Arntl*$^{-/-}$ mice, deletion of *Arntl* in white and brown adipocytes dampens the rhythmic expression of *Nr1d1* and *Per3* in WAT ($P < 0.01$) (Fig. 1i) and *Per2*, *Per3* and *Dbp* in BAT ($P < 0.05$) (Fig. 1j). Because of the reduction in the expression of the repressor, *Nr1d1*, the expressions of *Npas2* and *Cry1* in WAT and BAT of these mice are higher compared to the same tissues in control mice ($P < 0.0001$)[23–25]. The lack of complete loss of oscillation of clock genes in WAT may reflect the function of remnant *Arntl* expression from the incomplete excision of the gene by Cre recombinase, as well as the existence of cells other than adipocytes in the tissue. Notably, the expression of *Per1* and *Per2* continues to be rhythmic with unaltered amplitude in the WAT of Ad-*Arntl*$^{-/-}$ mice, which suggests that *Per1* and *Per2* do not depend on the intrinsic circadian clock of the white adipocyte to oscillate. Oscillation of *Per2* expression independent of the intrinsic clock has been previously described in liver of mice with a dysfunctional liver clock[26–28]. *Per2* oscillates in liver in the absence of a functional liver clock but not in liver explants from the same mice, which indicates that *Per2* oscillation could be driven by circadian systemic signals[28]. Taken together, the changes in clock and clock-output gene expression in the WAT and BAT of Ad-*Arntl*$^{-/-}$ mice indicate that the function of the circadian oscillator in both white and brown adipocytes is severely compromised.

Obesity in Ad-*Arntl*$^{-/-}$ mice

To address the hypothesis that the circadian clock of the adipocyte is important for energy homeostasis, we investigated changes in the body weight of Ad-*Arntl*$^{-/-}$ mice. Ad-*Arntl*$^{-/-}$ mice show significantly higher body weight when maintained on regular diet compared to control and WT mice starting at 9 weeks of age ($P < 0.05$; Fig. 2a and Supplementary Fig. 2a). The Ad-*Arntl*$^{-/-}$ mice were born at normal weight, which is consistent with a failure of adipocyte Arntl to affect fetal development and growth. We next fed the mice a high-fat, energy-dense diet (HFD). The HFD-fed Ad-*Arntl*$^{-/-}$ mice (HFD started at 6 weeks of age) gained significantly more weight compared to control mice, *aP2*-Cre mice and WT mice ($P < 0.05$; Fig. 2a). By contrast, M-*Arntl*$^{-/-}$ mice fed either a regular diet or the HFD did not have higher body weight compared to control and WT mice (Supplementary Fig. 1e). Thus, the higher body weight in the Ad-*Arntl*$^{-/-}$ mice was caused by the deletion of *Arntl* in adipocytes and not macrophages.

We generated a second line of Ad-*Arntl*$^{-/-}$ mice by crossing mice carrying the conditional *Arntl* allele with mice expressing Cre recombinase under the control of the adiponectin gene promoter (adiponectin-Cre *Arntl*^{fx}; Supplementary Fig. 2b) further to confirm the diet-induced obesity of Ad-*Arntl*$^{-/-}$ mice[29]. The adiponectin-Cre *Arntl*^{fx} mice did not have higher body weight compared to controls when fed the regular diet but gained significantly more weight compared to controls when fed the HFD staring at 6 weeks of age (Fig. 2b), similarly to the Ad-*Arntl*$^{-/-}$ mice expressing Cre recombinase under the control of the *aP2* promoter ($P < 0.05$). Notably, the adiponectin-Cre controls had lower weight compared to *Arntl*^{fx} controls and littermate WT mice. The observed diet-induced obesity in two separate Ad-*Arntl*$^{-/-}$ models is consistent with the interpretation that the higher body weight is caused by adipocyte-specific deletion of *Arntl*. This higher body weight is attributable to a greater adipose tissue mass. Thus, body fat comprises ~20% of the body weight in 32-week-old Ad-*Arntl*$^{-/-}$ mice fed a regular diet compared to 16% in control mice, with no difference in the weight of lean tissue between Ad-*Arntl*$^{-/-}$ and control mice (Fig. 2c). Similar to the mice fed a regular diet, 16-week-old Ad-*Arntl*$^{-/-}$ mice fed a HFD had no difference in lean tissue weight but had ~50% more adipose tissue compared to control mice (Fig. 2c). Histological analysis revealed adipocyte hypertrophy in Ad-*Arntl*$^{-/-}$ mice. Adipocytes from regular diet–fed Ad-*Arntl*$^{-/-}$ mice were ~30% larger than adipocytes from control mice (Fig. 2d,e). The epididymal adipose tissue of the Ad-*Arntl*$^{-/-}$ mice had no differences in macrophage infiltration and degree of fibrosis compared to the same tissue from control mice (Supplementary Fig. 2c,d). Expression of *Emr1* (*F4/80*), *Tnfa* and *Il1b* in epididymal adipose tissue was not different between Ad-*Arntl*$^{-/-}$ and control mice (Supplementary Fig. 2e), suggesting that the inflammatory state of the adipose tissue from Ad-*Arntl*$^{-/-}$ mice is the same as in the control mice. *Ex vivo* stimulation of WAT from Ad-*Arntl*$^{-/-}$ mice with isoproterenol showed lower levels of lipolysis in response to beta-3 adrenergic stimulation compared to control mice (Supplementary Fig. 2f). The expression of adipose triglyceride lipase and hormone-sensitive lipase in adipose tissue of Ad-*Arntl*$^{-/-}$ mice was normal, indicating no change in lipolysis in the adipocytes (Supplementary Fig. 2g). In support of this, plasma concentrations of nonesterified fatty acids in Ad-*Arntl*$^{-/-}$mice were the same as in control mice (Supplementary Fig. 2h).

We found higher concentrations of plasma leptin in Ad-*Arntl*$^{-/-}$mice fed a regular diet compared to controls (Fig. 2f). This might be expected given the greater adipose tissue mass in Ad-*Arntl*$^{-/-}$ mice, as there is a positive correlation between plasma leptin and adipose tissue mass in both humans and rodents[30]. High concentrations of leptin serve as a satiety signal from adipose tissue to the hypothalamic centers regulating appetite[11], which might seem at odds with the obesity in the Ad-*Arntl*$^{-/-}$ mice. However, higher concentrations of systemic plasma leptin coincide with obesity in rodents and humans but are associated with diminished hypothalamic leptin signaling[31], a phenomenon described as hypothalamic leptin resistance. Apart from the difference in plasma concentrations, we did not detect an apparent rhythm in the concentration of plasma leptin in either Ad-*Arntl*$^{-/-}$ or control mice. The concentrations of both plasma triglycerides and glucose oscillate in regular diet–fed control mice, as we previously described[7]. Regular diet–fed Ad-*Arntl*$^{-/-}$ mice have higher concentrations of plasma triglycerides (Fig. 2f) but no differences in the concentrations of plasma cholesterol and adiponectin compared to control mice (Supplementary Fig. 3a). In addition, the circadian variation in plasma triglyceride concentrations in control mice was lost in Ad-*Arntl*$^{-/-}$ mice (Fig. 2f).

Previously, we have shown temporal variation in glucose tolerance and the hypoglycemic response to insulin in mice[7]. We were therefore interested to explore whether disruption of the circadian clock in adipocytes has an impact on glucose metabolism. Regular diet–fed Ad-*Arntl*$^{-/-}$ mice kept under constant darkness showed a peak in plasma glucose concentration during the subjective light period of the day-night cycle (Fig. 2f). WT mice

consume most of their daily food during the beginning of the night. Therefore, plasma glucose concentrations of WT mice rise during the early night and drop after the postprandial period to lower steady-state concentrations during the day. We observed this pattern of plasma glucose variation in control mice but found that it was disrupted in Ad-*Arntl*$^{-/-}$ mice (Fig. 2f). Ad-*Arntl*$^{-/-}$ mice showed no difference in plasma concentrations of insulin across the 24-h light-dark cycle compared to control mice (Supplementary Fig. 3a) and had a normal plasma glucose response to intraperitoneal injection of insulin when fed a regular diet or a HFD for 4 weeks or 18 weeks, respectively (Supplementary Fig. 3b), despite their higher body weight.

We performed hyperinsulinemic-euglycemic clamp studies in 1-year-old Ad-*Arntl*$^{-/-}$ mice fed a HFD for 40 weeks further to analyze glucose metabolism. Consistent with the results from the insulin tolerance tests, there was no difference in the glucose infusion rate required to maintain euglycemia between Ad-*Arntl*$^{-/-}$ and control mice (Supplementary Fig. 3c). In addition, the suppression in hepatic glucose production after insulin infusion, the rate of blood glucose disposal and the glucose uptake by skeletal muscle and adipose tissue were not different between Ad-*Arntl*$^{-/-}$ and control mice, despite the higher body weight of the Ad-*Arntl*$^{-/-}$ mice (Supplementary Fig. 3c). Consistent with the absence of a change in sensitivity of adipose tissue to insulin, insulin-stimulated phosphorylation of insulin receptor substrate 1 (IRS-1) and Akt were not different in epididymal adipose tissue from Ad-*Arntl*$^{-/-}$ mice compared to the same tissue from control mice (Supplementary Fig. 3d). We and others have reported that mice lacking *Arntl* function in all tissues have higher sensitivity to insulin[4,7]. Specific deletion showed that liver *Arntl* function is at least partially responsible for this effect[4]. Here we show that *Arntl* function in the adipocyte may also contribute to sensitivity to insulin, as adipose tissue from Ad-*Arntl*$^{-/-}$ mice is equally sensitive to insulin compared to adipose tissue from control mice despite the greater body adiposity.

Reduced energy expenditure, attenuated food intake rhythm

We analyzed several aspects of behavior relevant to energy homeosta-sis in preobese 20-week-old mice fed HFD for 1 week to evaluate the energy surplus responsible for the higher body weight in long-term HFD-fed Ad-*Arntl*$^{-/-}$ mice without the confounder of body weight (Supplementary Fig. 4a). Ad-*Arntl*$^{-/-}$ mice showed no changes in locomotor activity compared to controls (Fig. 3a,b). Similarly, the SCN of regular diet–fed Ad-*Arntl*$^{-/-}$ mice drove normal rhythms in locomotor activity measured for several consecutive days under both light-dark (Supplementary Fig. 4b,c) and constant darkness conditions (Supplementary Fig. 4d) using both infrared beam crossing and telemetry. Conversely, energy expenditure, measured by respiratory O_2 consumption, was lower in HFD-fed Ad-*Arntl*$^{-/-}$ mice compared to controls (Fig. 3c,d). This lower expenditure was independent of the time of the diurnal cycle, whereas energy expenditure in the Ad-*Arntl*$^{-/-}$ mice remained rhythmic (Fig. 3c). Energy expenditure in regular diet–fed Ad-*Arntl*$^{-/-}$ mice was the same as in controls (Supplementary Fig. 4e,f). Similarly, there were no differences in the expression of *Ucp1* or *Ppargc1a* (*Pgc*-1α),which encode key regulators of thermogenesis, in brown and WAT both in the fed and fasted states (Supplementary Fig. 5a – d). We found no differences in the expression of genes encoding other regulators of thermogenesis, making a change in thermogenesis in BAT unlikely (Supplementary Fig. 5e). Plasma concentrations of triiodothyronine (T3), a thyroid hormone that increases energy expenditure, were the same in regular diet–fed Ad-*Arntl*$^{-/-}$ and control mice (Supplementary Fig. 5f). We also measured heat production as an indicator of thermogenesis using indirect calorimetry and found no differences between Ad-*Arntl*$^{-/-}$and control mice (Supplementary Fig. 5g).

Taken together, our findings suggest that the reduction in energy expenditure in HFD-fed mice is not the direct result of disruption of the adipocyte clock but, rather, is a secondary

event. There is no indication that thermogenesis in the BAT is altered in Ad-*Arntl*$^{-/-}$mice, a potential confounder in our study given the deletion of *Arntl* in brown adipocytes. Monitoring of food intake in the Ad-*Arntl*$^{-/-}$mice revealed attenuation of the diurnal rhythm in feeding activity observed in WT mice. Our control mice consumed ~70% of their total daily calorie intake during the night (Fig. 3e,f). In contrast, the Ad-*Arntl*$^{-/-}$ mice had greater food intake during the light period and lower food intake during the night (~60% of the total daily intake) compared to control mice, with no difference in the overall calories consumed daily between the two groups (Fig. 3e,f).

We reproduced the greater food intake during the light period in Ad-*Arntl*$^{-/-}$ mice in several independent experiments, as well as in regular diet–fed mice under both light-dark (Supplementary Fig. 4g) and constant darkness conditions (Supplementary Fig. 4h). The peak in plasma glucose concentrations during the light period in the regular diet–fed Ad-*Arntl*$^{-/-}$ mice (Fig. 2f) may have been the result of greater food intake during that period. Although feeding behavior in humans is very different than that in rodents, the greater food intake during the light period in the nocturnal Ad-*Arntl*$^{-/-}$ mice is reminiscent of the night-eating syndrome described in humans. Similar to the higher body weight of Ad-*Arntl*$^{-/-}$ mice, night-eating syndrome is more prevalent in obese than lean humans[32].

Increased food intake during daytime leads to obesity

We restricted Ad-*Arntl*$^{-/-}$ mice access to food either during the light or the dark period to examine whether the greater feeding activity during the light period without an overall increase in daily food intake underlies the diet-induced obesity in these mice. We provided the same number of daily calories to mice in the restricted feeding groups and a group with *ad libitum* access to food and monitored their weight for several days. After an initial adjustment period (days 1–17) that allowed the mice to adapt to the time-restricted access to food, mice in the three groups had no differences in body weight (Fig. 4a). We then introduced the mice to a HFD. Mice fed during the light period gained significantly more weight and were heavier compared to mice fed during the dark period throughout the experiment ($P < 0.05$; Fig. 4a). This indicates that the attenuated feeding behavior of Ad-*Arntl*$^{-/-}$ mice is sufficient to lead to obesity without an overall increase in daily caloric intake.

We next investigated whether the disruption of the clock in adipocytes changed the adipose–central nervous system axis that regulates feeding behavior. We analyzed the hypothalamic expression of neuropeptides involved in appetite regulation in preobese mice fed a regular diet (Supplementary Fig. 6a,b). In agreement with the increase in food intake, we found higher expression of orexigenic neuropeptide Y (*Npy*) and agouti related peptide (*Agrp*) in Ad-*Arntl*$^{-/-}$ mice compared to controls specifically at circadian time 4 (CT4) of the subjective light period (Fig. 4b,c), which corresponds to the time when Ad-*Arntl*$^{-/-}$ mice consume more food than controls (Fig. 3e,f). In addition, we found higher expression of the orexin receptor 2 (*Hcrtr2*) in Ad-*Arntl*$^{-/-}$ mice at CT0 and CT4 compared to controls (Fig. 4d). By contrast, expression of the anorexigenic cocaine and amphetamine-regulated transcript (*Cart*) was lower in Ad-*Arntl*$^{-/-}$ than control mice at CT4 (Fig. 4e). The expression of both orexigenic and anorexigenic neuropeptides was the same in Ad-*Arntl*$^{-/-}$ and control mice at all other times of the daily cycle (Fig. 4b – f). We found no differences in the expression of pro-opiomelanocortin (*Pomc*) (Fig. 4f) or other regulators of feeding behavior, such as the leptin receptor, orexin or orexin receptor 1, between the two groups (Supplementary Fig. 6c). We examined the expression of clock and clock-output genes in the hypothalamus of the same mice to exclude the possibility that the changes in neuropeptide expression resulted from changes in hypothalamic clock function (Supplementary Fig. 6d). Clock and clock-output genes showed low amplitude oscillations in the hypothalamus, with no differences between Ad-*Arntl*$^{-/-}$ and control mice

(Supplementary Fig. 6d). Taken together, these findings indicate a temporal change in appetite that dictates the attenuation of the feeding behavior of the Ad-*Arntl*$^{-/-}$ mice.

We fasted mice for 24 h and monitored their response to refeeding as a second test for changes in the adipose–central nervous system axis that regulates feeding behavior. After refeeding, Ad-*Arntl*$^{-/-}$ mice showed greater food intake compared to control mice (Fig. 4g). The same response was evident 2 h after the start of refeeding. Our finding indicates a greater appetite in response to a lack of energy, suggesting a higher set point for energy stored in the adipose tissue of the Ad-*Arntl*$^{-/-}$ mice. Ad-*Arntl*$^{-/-}$ mice also had greater food intake compared to controls 13, 15, 17 and 19 h after the initiation of refeeding (Fig. 4g). The greater intake at these hours is probably related to the higher food intake of Ad-*Arntl*$^{-/-}$ mice during the light period.

Reduced polyunsaturated fatty acids in Ad-*Arntl*$^{-/-}$ mice

We next investigated changes in the adipocytes of Ad-*Arntl*$^{-/-}$ mice that initiate the attenuated feeding behavior that leads to obesity. We performed a metabolomic analysis in epididymal adipose tissue collected from regular diet–fed 20-week-old mice at different times of the diurnal cycle (CT0, CT6, CT12 and CT18) and found opposing changes between the concentration of triglycerides containing saturated, monounsaturated and polyunsaturated fatty acids (Fig. 5a,b). The concentration of triglycerides TG (52:0), TG (51:1), TG (52:1), TG (53:1) and TG (54:1) was higher in Ad-*Arntl*$^{-/-}$ compared to control mice (Fig. 5a). Conversely, the concentration of triglycerides TG (50:3), TG (50:4), TG (52:5), TG (54:8), TG (58:8) and TG (56:9) was lower in Ad-*Arntl*$^{-/-}$ compared to control mice (Fig. 5b). To explain the observed changes, we performed a genome-wide microarray analysis of the epididymal adipose tissue. Expression of *Elovl6*, encoding long-chain fatty acid elongase 6 (responsible for lengthening the carbon chain during biosynthesis of long-chain polyunsaturated fatty acids), and *Scd1*, encoding stearoyl-CoA desaturase 1 (which creates a double bond at the ninth position of the fatty acid carbon chain during polyunsaturated fatty acid biosynthesis), was lower in Ad-*Arntl*$^{-/-}$ compared to control mice (Fig. 5c). *Elovl6* and *Scd1* contain E-boxes in their promoter regions, suggesting direct control of their expression by the circadian clock[33]. To confirm the regulation of *Elovl6* and *Scd1* expression by Arntl, we used chromatin immunopre-cipitation (ChIP), quantitative PCR and found that Arntl associates with the E-boxes of the promoter regions of the two genes (Fig. 5d). The lower expression of *Elovl6* and *Scd1* indicates a lower capacity of Ad-*Arntl*$^{-/-}$ adipocytes to synthesize long-chain polyunsaturated fatty acids compared to control adipocytes and explains the lower abundance of triglycerides containing polyunsaturated fatty acids in Ad-*Arntl*$^{-/-}$ mice.

The differences in triglyceride abundances in the adipose tissue of Ad-*Arntl*$^{-/-}$ mice compared to control mice prompted us to measure fatty acids in the plasma from the mice in the same experiment. Adipose tissue releases fatty acids into the circulation for use by other tissues for energy production through fatty acid oxidation or to serve as receptor ligands[34]. Long-chain polyunsaturated fatty acids cross the blood-brain barrier and incorporate into neurons of hypothalamic centers that regulate food intake among other cells and regions of the brain[14]. Low concentrations of polyunsaturated fatty acids in the hypothalamus associate with higher food intake in rats, and an increase of polyunsaturated fatty acid concentration leads to reduced feeding activity[16]. Plasma concentrations of saturated fatty acids are higher in Ad-*Arntl*$^{-/-}$ compared to control mice (Fig. 5e). In contrast, the concentrations of unsaturated fatty acids in plasma from Ad-*Arntl*$^{-/-}$ mice are lower compared to controls (Fig. 5f,g). More specifically, the concentrations of arachidonic acid, eicosapentaenoic acid (EPA) and docosahexaenoic acid (DHA) are lower in Ad-*Arntl*$^{-/-}$ than control mice at CT6, corresponding to the time Ad-*Arntl*$^{-/-}$ mice have greater food intake compared to controls (Fig. 5g). Our findings suggest that the lower concentration of plasma long-chain

polyunsaturated fatty acids in Ad-*Arntl*$^{-/-}$ mice at CT6 should be reflected in the concentration of polyunsaturated fatty acids in hypothalamic neurons, causing greater food intake in the knockout mice at that time.

We next sought changes in gene expression in the adipose tissue of Ad-*Arntl*$^{-/-}$ mice that might explain how a lower concentration of adipose tissue polyunsaturated fatty acid containing triglycerides results in a lower plasma concentration of polyunsaturated fatty acids specifically at CT6. Expression of *Ces1d*, encoding triacylglycerol hydrolase, is lower in adipose tissue of Ad-*Arntl*$^{-/-}$ mice compared to the same tissue from controls specifically at CT6 (Fig. 5h). *Ces1d* contains E-boxes in its promoter region, consistent with control of its expression by the circadian clock. Triacylglycerol hydrolase is a major adipocyte lipase that was recently found to be responsible for approximately 70% of the total hydrolase activity in WAT[35]. The lower expression of *Ces1d* in Ad-*Arntl*$^{-/-}$ mice at CT6 indicates less lipolysis in WAT of these mice at that time compared to controls. Less lipolysis leads to less release of fatty acids in plasma and explains the lower plasma concentrations of polyunsaturated fatty acids at CT6. We measured arachidonic acid, EPA and DHA in the hypothalamus of Ad-*Arntl*$^{-/-}$ mice to explore whether the time-specific reduction in the concentration of polyunsaturated fatty acids in plasma changes the concentrations of polyunsaturated fatty acids in hypothalamic neurons. The concentration of hypothalamic nonesterified arachidonic acid, EPA and DHA are lower in Ad-*Arntl*$^{-/-}$ mice compared to controls specifically at CT6 (Fig. 5i). Conversely, the concentrations of esterified arachidonic acid and DHA are the same in the Ad-*Arntl*$^{-/-}$mice and controls (Supplementary Fig. 7a), which is consistent with the temporal reduction of polyunsaturated fatty acids in plasma. The concentration of esterified EPA was lower in the hypothalamus of Ad-*Arntl*$^{-/-}$ mice at CT6 compared to control mice (Supplementary Fig. 7a). Our findings suggest that the lower concentration of circulating polyunsaturated fatty acids during the light period cause a reduction in the concentration of nonesterified polyunsaturated fatty acids in the hypothalamus at the same time. This reduction may change hypothalamic neuropeptide expression to promote greater food intake during the light period.

Peripheral polyunsaturated fatty acids: energy homeostasis

To determine whether the lower concentration of circulating polyun-saturated fatty acids during the light period causes increased feeding and leads to increased body weight, we fed Ad-*Arntl*$^{-/-}$ mice two diets with high polyunsaturated fatty acid contents. The first diet provided 2% of its energy from EPA and DHA (1.2% EPA and 0.8% DHA), and the second diet provided 10% of its energy from EPA and DHA (6% EPA and 4% DHA), with 43% of the total energy being provided from fat in both diets. Feeding the mice the 2% EPA and DHA diet led to lower amounts of arachidonic acid and higher amounts of EPA in the hypothalamus compared to mice fed a control diet with 43% of the total energy from fat (HFD) (Fig. 6a and Supplementary Fig. 7b). The 10% EPA and DHA diet led to lower amounts of arachidonic acid and higher amounts of EPA and DHA in the hypothalamus compared to mice fed the HFD (Fig. 6a and Supplementary Fig. 7b). The difference in the amount of nonesterified arachidonic acid, EPA and DHA at CT4 between Ad-*Arntl*$^{-/-}$and control mice fed the HFD disappeared after feeding the mice with the two EPA- and DHA-rich diets (Fig. 6a). Consistent with the hypothesis that lower concentrations of circulating polyunsaturated fatty acids during the light period are responsible for the increase in body weight, the Ad-*Arntl*$^{-/-}$ mice fed the two EPA- and DHA-rich diets did not have higher body weight compared to the control mice (Fig. 6b). Feeding the Ad-*Arntl*$^{-/-}$ mice the EPA- and DHA-rich diets corrected the greater food intake during light period in the HFD-fed Ad-*Arntl*$^{-/-}$ mice (Fig. 6c). Energy expenditure in the Ad-*Arntl*$^{-/-}$ mice fed the EPA- and DHA-rich diets was equal to that of the control mice (Fig. 6d). The locomotor activity of the Ad-*Arntl*$^{-/-}$ mice was the same as the control mice in both the HFD and the EPA- and DHA-

rich diet groups (Supplementary Fig. 7c). These findings indicate that the elimination of the low amounts of polyunsaturated fatty acids in the hypothalamus by supplementation of the diet with EPA and DHA restores body weight, feeding behavior and energy expenditure in the Ad-*Arntl*$^{-/-}$ mice.

We then measured the expression of hypothalamic neuropeptides that regulate feeding activity to test the hypothesis that low amounts of hypothalamic polyunsaturated fatty acids in Ad-*Arntl*$^{-/-}$ mice change feeding activity by changing neuropeptide expression. HFD-fed Ad-*Arntl*$^{-/-}$ mice have higher expression of *Npy* and *Agrp* and lower expression of *Cart* and *Pomc* in the hypothalamus at CT4 compared to HFD-fed control mice (Fig. 6e). The expressions of leptin receptor, orexin, and orexin receptors 1 and 2 at CT4 were the same between Ad-*Arntl*$^{-/-}$ and control mice (Supplementary Fig. 7d). Supplementation of the diet of Ad-*Arntl*$^{-/-}$ mice with EPA and DHA reduced the expression of *Npy* and *Agrp* and increased the expression of *Cart* and *Pomc* at CT4 to the expressions in the control mice (Fig. 6e). Our findings indicate that the changes in hypothalamic neuropeptides in Ad-*Arntl*$^{-/-}$ mice are caused by the lower amounts of hypothalamic polyunsaturated fatty acids (Supplementary Fig. 8).

DISCUSSION

Our study provides evidence that a peripheral circadian clock can generate circadian signals to entrain rhythmicity in the central nervous system. Disruption of adipocyte clock function results in temporal changes in plasma concentration of polyunsaturated fatty acids, leading to corresponding changes in the expression of neurotransmitters responsible for appetite regulation in hypothalamic feeding centers. The magnitude of the effect on hypothalamic expression of neurotransmitters is sufficient to induce changes in feeding activity, as previously described[36,37], leading to disruption of the normal feeding rhythm. These changes occur without alteration in the rhythmic expression of circadian clock genes (including *Arntl*) in the hypothalamus, suggesting a direct effect of the adipocyte circadian clock on hypothalamic feeding centers without the participation of the local circadian clocks. This finding suggests a bidirectional communication between the SCN and peripheral clocks. Recently, regulation of SCN synchronization by adrenal glucocorticoids was reported in a mouse model of jet lag[38]. Disruption of the adrenal circadian clock and circadian rhythm in glucocorticoid secretion alters the kinetics of the SCN-controlled locomotor activity rhythm re-entrainment[38].

The development of obesity in Ad-*Arntl*$^{-/-}$ mice highlights the importance of the adipocyte circadian clock in organismal energy homeostasis. Deletion of *Arntl* in adipocytes results in weight gain, an effect that is not observed with deletion of *Arntl* in the liver[4] or pancreatic islets[3]. Together with the temporal alterations in the concentration of plasma and hypothalamic polyunsaturated fatty acids and in hypothalamic neurotransmitters, our finding suggests an underlying dysfunction of the clock and not a direct effect of Arntl. Healthy adult mammals maintain a steady body weight over most of their lives, which suggests that energy homeostasis is a tightly regulated process. Lipolysis in WAT releases energy stored in adipocytes. In turn, adipocytes signal the amount of stored energy to the hypothalamus, a key input to the centers responsible for energy homeostasis. The alterations in feeding activity—a centrally mediated behavior—in mice with adipocyte-specific disruption of the clock indicate feedback from a peripheral clock to the central nervous system. The adipocyte clock regulates the biosynthesis of long-chain polyunsaturated fatty acids and the timing of fatty acid release into the circulation. Remodeling of the triglyceride pool of the adipocyte in the absence of a functional clock leads to an attenuated feeding rhythm and obesity. Indeed, obesity in humans has been associated with remodeling of the adipocyte lipidome that is characterized by a reduction in the amount of polyunsaturated fatty acids[39]. Disruption of

the circadian clock in adipocytes results in a reduction in the amount of key enzymes involved in the biosynthesis of polyunsaturated fatty acids, explaining the reduced amounts of polyunsaturated fatty acid containing triglycerides. This, together with a time-specific reduction in triacylglycerol hydrolase, results in a reduction in the amount of plasma long-chain polyunsaturated fatty acids during the light period of the diurnal cycle. Reflecting the transit of polyunsaturated fatty acids from plasma across the blood-brain barrier, the amounts of nonesterified polyunsaturated fatty acids in the hypothalamic centers regulating feeding activity are also reduced during the light period.

Previous studies have shown that dysregulation of the feeding rhythm without an increase in total food intake can lead to obesity in rodents[40–45]. Restriction of food availability only to the light phase induces accelerated obesity in mice fed a HFD compared to mice with access to food only during the night that consume the same number of calories[40]. Furthermore, correction of the abnormal feeding rhythm by scheduled feeding rescues the onset of obesity in HFD-fed mice[41,42] and in a genetic model of hyperphagia with a dysregulated feeding rhythm[43]. In a model of shift work, mice with restricted access to food during the light phase develop obesity. Shifting food access to the night phase reverses this weight gain[44]. Similarly, exposure of mice to light during the night results in obesity as a result of a shift of food intake to the light phase[45]. In humans, dysregulation of feeding and sleep rhythms in a paradigm of circadian misalignment results in a reduction of the amount of plasma leptin that would predispose to the development of obesity[46]. Similar to our findings, HFD-fed mice with an attenuated feeding rhythm show reduced energy expenditure, and correction of the feeding rhythm results in an increase of energy expenditure[41,42]. These observations suggest that attenuation of the feeding rhythm shifts energy toward storage instead of utilization, as indicated by a reduction in energy expenditure.

Polyunsaturated fatty acids in the hypothalamus improve hypothalamic signaling of leptin and insulin by reducing hypothalamic inflammation[16]. As we show with the use of diets rich in EPA and DHA, the release of these lipids from adipose tissue to the circulation can serve as a peripheral signal to the hypothalamus to regulate feeding. Hypothalamic amounts of polyunsaturated fatty acids oscillate, with a peak during the light period of the diurnal cycle. When the adipocyte clock is disrupted, circulating polyunsaturated fatty acid concentrations are low during the light period, resulting in reduced amounts of hypothalamic polyunsaturated fatty acids and increased feeding activity at a time when feeding is normally low. Increased food intake at an inappropriate time leads to obesity through a shift of energy toward storage and a reduction in energy expenditure[41,42]. Our study provides evidence for the importance of timing as a modulator of the adipocyte-hypothalamic axis and its impact on body weight. Both short-term and long-term signals participate in the regulation of energy homeostasis. Our findings show that short-term changes have an immediate effect on food intake rhythmicity. Over time, the changes in rhythmic food intake lead to an increase in body weight.

ONLINE METHODS

Mice and tissue collection

A single *loxP* site and a Neo cassette flanked by an additional *loxP* site and two Frt sites were introduced into the introns upstream and downstream of coding exon 4 in mice bearing a conditional *Arntl*^{fx} allele. Mice were euthanized under infrared light for tissue collection under circadian time. Tissues were dissected under light and frozen immediately in liquid nitrogen. Mice on a high-fat diet were fed a diet in which 43% of the calories came from fat (Harlan Laboratories Inc., Teklad TD.88137). Studies were performed in accordance with the protocol approved by the University of Pennsylvania Institutional Animal Care and Use Committee. Mouse genotypes were assessed by PCR on genomic DNA from tail tips.

Real-time PCR

Total RNA was isolated from tissues using Qiagen RNeasy Mini Kit. Reverse transcription was achieved using a Transcriptor First-Strand cDNA Synthesis Kit (Roche). The sequences of the primer pairs are listed in the Supplementary Methods. Quantitative PCR was done on a 7900HT Real-Time PCR System (Applied Biosystems) using SYBR Green. Levels were normalized against Gapdh.

Western blot

For the detection of Arntl, freshly prepared primary adipocytes were lysed in buffer containing protease inhibitors. Arntl detection was carried out by SDS-PAGE. A primary antibody to Arntl (Bethyl Laboratories Inc., A302–616A) was used at a dilution of 1:500, and a donkey rabbit-specific secondary antibody was used at 1:2,000 (Jackson ImmunoResearch Laboratories Inc., 711-035–152). For the detection of phosphorylated IRS-1 and Akt, 20-week-old mice were fasted for 16 h, injected intraperitoneally with saline or insulin at 10 units per kg of body weight and euthanized 30 min later. Total protein was prepared from epididymal adipose tissue. Primary antibodies to IRS-1 (Millipore, 06–248), IRS-1 phosphory-lated at Tyr612 (pTyr612) (Invitrogen, 44–816G), Akt (Cell Signaling, 9272) and Akt pThr308 (Cell Signaling, 9275) were used at dilutions of 1:500, 1:750, 1:1,000 and 1:750, respectively. β-actin (Sigma, A5441) was used as a loading control.

Body composition

Body composition of the mice was analyzed by dual energy X-ray absorptiometry (Lunar, PIXImus).

Measurement of plasma leptin, adiponectin, triglycerides, total cholesterol, T3, insulin and glucose

Leptin was measured by ELISA (R&D Systems, MOB00), adiponectin was measured by ELISA (R&D Systems, MRP300), triglycerides were measured by a calorimetric assay (Wako Diagnostics, 997–37492), total cholesterol was measured by a calorimetric assay (Wako Diagnostics, 439–17501), T3 was measured by ELISA (Calbiotech, T3043T-100), insulin was measured by ELISA (Crystal Chem, 90080), and glucose was measured with a Contour blood glucometer with disposable test strips (Bayer).

Histological analysis

Adipocyte size was quantified in 5-μm sections of epididymal adipose tissues stained with H&E. Individual cell area was quantified in five random sections per mouse. Adipocyte size was calculated as the average of five mice per group. Immunohistochemistry for F4/80 was performed in sections of epididymal adipose tissue incubated with an F4/80-specific antibody (Invitrogen, MF48000) at a dilution of 1:20 for 2 h at room temperature. A rat IgG-specific secondary antibody (Vector Laboratories, BA-4001) was used at a 1:200 dilution for 30 min at room temperature.

Behavioral and calorimetric analysis

Locomotor activity, vO_2, heat production and food intake were measured at a consistent environmental temperature (22 °C) using an indirect calorimetry system (Oxymax Comprehensive Lab Animal Monitoring System, Columbus Instruments, Columbus, OH). For mice, studies were commenced after 48 h of acclimatization to the metabolic chamber. During the studies, mice had *ad libitum* access to food and water. Locomotor activity was measured as the number of breaks of laser beams running the mouse cage by the mouse body as the mouse moves.

Insulin tolerance test and hyperinsulinemic-euglycemic clamp

Mice were fasted for 6 h and then injected intraperitoneally with insulin (1 U per kg of body weight), and blood glucose concentrations were monitored over time using a Contour blood glucometer (Bayer). Mice were cannulated in the lateral cerebral ventricle and catheterized in the right internal jugular vein for the hyperinsulinemic-euglycemic clamp. Details of the test are provided in the Supplementary Methods.

Isolation of hypothalamic sections

Hypothalamic sections were taken as described previously[47]. In short, the brains were rapidly removed, and five cuts were made using a razor blade. Viewing the ventral side of the brain, two coronal cuts were placed at the apex of the optic chiasm and the rostral margin of the mammillary bodies. This slab was then placed flat, and two cuts were placed on either side of the optic chiasm. A third cut was placed just above the third ventricle.

Ex vivo lipolysis

Epididymal fat pads were surgically removed, washed three times with PBS and cut into 20-mg pieces. The tissue was incubated in a humidified atmosphere of 5% CO_2 and 95% O_2 at 37 °C in DMEM (Invitrogen, 21063-029) containing 2% fatty acid–free BSA (Calbiochem, 123575) with or without 10 μM isoproterenol (Sigma, I6504) for 4 h. The concentrations of nonesterified fatty acids and glycerol were determined in the medium using calorimetric assays (Wako, 999–34691 and Sigma, FG0100). Values were corrected for the amount of total protein.

LC-MS

LC-MS was performed on blood plasma and the lipid fraction of the epididymal adipose tissue using a Thermo Scientific Exactive Orbitrap according to the method described by Roberts *et al.*[48], and metabolite identifications were confirmed by reference to databases (http://www.lipidmaps.org/) and the use of tandem mass spectrometry to obtain fragmentation patterns. In addition, the adipose tissue was analyzed by a Waters QToF Xevo using a Waters Ultra Performance Liquid Chromatograph (UPLC) and T3 column to provide chromatographic separation of lipid species. The resulting data were processed by the multivariate statistical algorithm of partial least squares discriminant analysis (PLS-DA). Fatty acids in hypothalamic tissue were measured by a Waters Xevo TQS using a Waters Acquity UPLC and an Acquity BEH C18 (150 mm × 2.1 mm × 1.7 μm) column to provide chromatographic separation of lipid species.

Microarray analysis

Samples were prepared in one batch using the Nugen sample preparation protocol and hybridized to Affymetrix Mouse array MoGene 1.0.st.v1. Data from the CEL files were summarized and normalized using RMA Express[49]. Twelve control and 12 Ad-*Arntl*$^{-/-}$ assays were used for a two-group differential expression analysis using a permutation *t* statistic–based method with a false discovery rate multiple testing correction[50]. Briefly, given a set S of *N* genes each with false discovery rate *p*, the expected number of false positives in S is *pN*.

ChIP

Epididymal WAT was harvested immediately after euthanasia at ZT10. It was quickly minced and crosslinked in 1% formaldehyde for 20 min, followed by quenching with 1/20 volume of 2.5 M glycine solution and two washes with 1× PBS. Nuclear extracts with fragmented chromatin were prepared by sonication in ChIP dilution buffer (50 mM HEPES, 155 mM NaCl, 1.1% Triton X-100, 0.11% sodium deoxycholate, 0.1% SDS, 1 mM PMSF

and complete protease inhibitor tablet, pH 7.5). Proteins were immunoprecipitated in ChIP dilution buffer using Arntl-specific antibody at a dilution of 1:100 (Bethyl, A302–616A). Crosslinking was reversed overnight at 65 °C in elution buffer (50 mM Tris-HCl, 10 mM EDTA and 1% SDS, pH 8), and DNA was isolated using phenol:chloroform:isoamyl alcohol. Precipitated DNA was analyzed by quantitative PCR. The primer sequences used were as follows: insulin forward 5′-GGACCCACAAGTGGAACAAC-3′, reverse 5′-GTG CAGCACTGATCCACAAT-3′; *Arbp* forward 5′-GAGGTGGCTTTGAA CCAGAG-3′, reverse 5′-TCTTTGTCTCTGTCTCGGAAAA-3′, *Scd1* forward 5′-TTGCTAAGCGCCAGACCAAAGT-3′, reverse 5′-GTGGGCTGATGGGT GACTTTTCTT-3′; *Elovl6* forward 5′-CCCAGGTCCTCATCCTCAGCAT CC-3′, reverse 5′-GGCAGCTTGGGCGCGGATTT-3′.

Statistical analyses

All direct comparisons were performed with a two-sample *t* test (parametric when the variables passed normality testing and Mann-Whitney otherwise). Testing for an absolute difference in levels across time was done by pooling, for each genotype, all measurements from all time points. The dampening of the rhythmic expression of clock genes was tested using a permutation test. The details of the analysis are provided in the Supplementary Methods.

Additional methods

Detailed methodology is described in the Supplementary Methods.

Supplementary Material

Refer to Web version on PubMed Central for supplementary material.

Acknowledgments

This work was supported by US National Institutes of Health (NIH) grant RO1 HL097800 and Medical Research Council grant UD99999906. We thank M. Lazar for help with the ChIP experiments (funded by NIH R01 DK45586). We thank R. Ahima and the Mouse Phenotyping, Physiology and Metabolism Core of the Penn Diabetes Research Center (P30 DK19525) for performing body composition and behavioral analysis; D. Baldwin's Microarray Core Facility for performing the microarray analysis; and R. Freer and M. Adam for technical assistance. G.A.F. is the McNeil Professor of Translational Medicine and Therapeutics.

References

1. Green CB, Takahashi JS, Bass J. The meter of metabolism. Cell. 2008; 134:728–742. [PubMed: 18775307]
2. Reppert SM, Weaver DR. Coordination of circadian timing in mammals. Nature. 2002; 418:935–941. [PubMed: 12198538]
3. Marcheva B, et al. Disruption of the clock components CLOCK and BMAL1 leads to hypoinsulinaemia and diabetes. Nature. 2010; 466:627–631. [PubMed: 20562852]
4. Lamia KA, Storch KF, Weitz CJ. Physiological significance of a peripheral tissue circadian clock. Proc. Natl. Acad. Sci. USA. 2008; 105:15172–15177. [PubMed: 18779586]
5. Oishi K, et al. Disrupted fat absorption attenuates obesity induced by a high-fat diet in Clock mutant mice. FEBS Lett. 2006; 580:127–130. [PubMed: 16343493]
6. Turek FW, et al. Obesity and metabolic syndrome in circadian Clock mutant mice. Science. 2005; 308:1043–1045. [PubMed: 15845877]
7. Rudic RD, et al. BMAL1 and CLOCK, two essential components of the circadian clock, are involved in glucose homeostasis. PLoS Biol. 2004; 2:e377. [PubMed: 15523558]
8. Ellingsen T, Bener A, Gehani AA. Study of shift work and risk of coronary events. J. R. Soc. Promot. Health. 2007; 127:265–267. [PubMed: 18085071]

9. Karlsson B, Knutsson A, Lindahl B. Is there an association between shift work and having a metabolic syndrome? Results from a population based study of 27,485 people. Occup. Environ. Med. 2001; 58:747–752. [PubMed: 11600731]
10. Spiegel K, Tasali E, Leproult R, Van Cauter E. Effects of poor and short sleep on glucose metabolism and obesity risk. Nat. Rev. Endocrinol. 2009; 5:253–261. [PubMed: 19444258]
11. Ahima RS, et al. Role of leptin in the neuroendocrine response to fasting. Nature. 1996; 382:250–252. [PubMed: 8717038]
12. Cowley MA, et al. Leptin activates anorexigenic POMC neurons through a neural network in the arcuate nucleus. Nature. 2001; 411:480–484. [PubMed: 11373681]
13. Mizuno TM, Mobbs CV. Hypothalamic agouti-related protein messenger ribonucleic acid is inhibited by leptin and stimulated by fasting. Endocrinology. 1999; 140:814–817. [PubMed: 9927310]
14. Lam TK, et al. Hypothalamic sensing of circulating fatty acids is required for glucose homeostasis. Nat. Med. 2005; 11:320–327. [PubMed: 15735652]
15. Pocai A, et al. Restoration of hypothalamic lipid sensing normalizes energy and glucose homeostasis in overfed rats. J. Clin. Invest. 2006; 116:1081–1091. [PubMed: 16528412]
16. Cintra DE, et al. Unsaturated fatty acids revert diet-induced hypothalamic inflammation in obesity. PLoS ONE. 2012; 7:e30571. [PubMed: 22279596]
17. Bunger MK, et al. Mop3 is an essential component of the master circadian pacemaker in mammals. Cell. 2000; 103:1009–1017. [PubMed: 11163178]
18. Bunger MK, et al. Progressive arthropathy in mice with a targeted disruption of the Mop3/Bmal-1 locus. Genesis. 2005; 41:122–132. [PubMed: 15739187]
19. Kondratov RV, Kondratova AA, Gorbacheva VY, Vykhovanets OV, Antoch MP. Early aging and age-related pathologies in mice deficient in BMAL1, the core component of the circadian clock. Genes Dev. 2006; 20:1868–1873. [PubMed: 16847346]
20. Westgate EJ, et al. Genetic components of the circadian clock regulate thrombogenesis *in vivo* . Circulation. 2008; 117:2087–2095. [PubMed: 18413500]
21. He W, et al. Adipose-specific peroxisome proliferator-activated receptor y knockout causes insulin resistance in fat and liver but not in muscle. Proc. Natl. Acad. Sci. USA. 2003; 100:15712–15717. [PubMed: 14660788]
22. Clausen BE, Burkhardt C, Reith W, Renkawitz R, Forster I. Conditional gene targeting in macrophages and granulocytes using LysMcre mice. Transgenic Res. 1999; 8:265–277. [PubMed: 10621974]
23. Etchegaray JP, Lee C, Wade PA, Reppert SM. Rhythmic histone acetylation underlies transcription in the mammalian circadian clock. Nature. 2003; 421:177–182. [PubMed: 12483227]
24. Ueda HR, et al. System-level identification of transcriptional circuits underlying mammalian circadian clocks. Nat. Genet. 2005; 37:187–192. [PubMed: 15665827]
25. Crumbley C, Wang Y, Kojetin DJ, Burris TP. Characterization of the core mammalian clock component, NPAS2, as a REV-ERBα/RORα target gene. J. Biol. Chem. 2010; 285:35386–35392. [PubMed: 20817722]
26. Debruyne JP, et al. A clock shock: mouse CLOCK is not required for circadian oscillator function. Neuron. 2006; 50:465–477. [PubMed: 16675400]
27. Miller BH, et al. Circadian and CLOCK-controlled regulation of the mouse transcriptome and cell proliferation. Proc. Natl. Acad. Sci. USA. 2007; 104:3342–3347. [PubMed: 17360649]
28. Kornmann B, Schaad O, Bujard H, Takahashi JS, Schibler U. System-driven and oscillator-dependent circadian transcription in mice with a conditionally active liver clock. PLoS Biol. 2007; 5:e34. [PubMed: 17298173]
29. Eguchi J, et al. Transcriptional control of adipose lipid handling by IRF4. Cell Metab. 2011; 13:249–259. [PubMed: 21356515]
30. Maffei M, et al. Leptin levels in human and rodent: measurement of plasma leptin and ob RNA in obese and weight-reduced subjects. Nat. Med. 1995; 1:1155–1161. [PubMed: 7584987]

31. El-Haschimi K, Pierroz DD, Hileman SM, Bjorbaek C, Flier JS. Two defects contribute to hypothalamic leptin resistance in mice with diet-induced obesity. J. Clin. Invest. 2000; 105:1827–1832. [PubMed: 10862798]
32. Stunkard A, et al. Binge eating disorder and the night-eating syndrome. Int. J. Obes. Relat. Metab. Disord. 1996; 20:1–6. [PubMed: 8788315]
33. Hogenesch JB, Gu YZ, Jain S, Bradfeld CA. The basic-helix-loop-helix-PAS orphan MOP3 forms transcriptionally active complexes with circadian and hypoxia factors. Proc. Natl. Acad. Sci. USA. 1998; 95:5474–5479. [PubMed: 9576906]
34. Oh DY, et al. GPR120 is an omega-3 fatty acid receptor mediating potent antiinflammatory and insulin-sensitizing effects. Cell. 2010; 142:687–698. [PubMed: 20813258]
35. Wei E, et al. Loss of TGH/Ces3 in mice decreases blood lipids, improves glucose tolerance, and increases energy expenditure. Cell Metab. 2010; 11:183–193. [PubMed: 20197051]
36. Minokoshi Y, et al. AMP-kinase regulates food intake by responding to hormonal and nutrient signals in the hypothalamus. Nature. 2004; 428:569–574. [PubMed: 15058305]
37. Ropelle ER, et al. IL-6 and IL-10 anti-inflammatory activity links exercise to hypothalamic insulin and leptin sensitivity through IKKβ and ER stress inhibition. PLoS Biol. 2010; 8:e1000465. [PubMed: 20808781]
38. Kiessling S, Eichele G, Oster H. Adrenal glucocorticoids have a key role in circadian resynchronization in a mouse model of jet lag. J. Clin. Invest. 2010; 120:2600–2609. [PubMed: 20577050]
39. Pietiläinen KH, et al. Association of lipidome remodeling in the adipocyte membrane with acquired obesity in humans. PLoS Biol. 2011; 9:e1000623. [PubMed: 21666801]
40. Arble DM, Bass J, Laposky AD, Vitaterna MH, Turek FW. Circadian timing of food intake contributes to weight gain. Obesity (Silver Spring). 2009; 17:2100–2102. [PubMed: 19730426]
41. Stucchi P, et al. Circadian feeding drive of metabolic activity in adipose tissue and not hyperphagia triggers overweight in mice: is there a role of the pentose-phosphate pathway? Endocrinology. 2012; 153:690–699. [PubMed: 22147018]
42. Hatori M, et al. Time-restricted feeding without reducing caloric intake prevents metabolic diseases in mice fed a high-fat diet. Cell Metab. 2012; 15:848–860. [PubMed: 22608008]
43. Masaki T, et al. Involvement of hypothalamic histamine H1 receptor in the regulation of feeding rhythm and obesity. Diabetes. 2004; 53:2250–2260. [PubMed: 15331534]
44. Salgado-Delgado R, Angeles-Castellanos M, Saderi N, Buijs RM, Escobar C. Food intake during the normal activity phase prevents obesity and circadian desynchrony in a rat model of night work. Endocrinology. 2010; 151:1019–1029. [PubMed: 20080873]
45. Fonken LK, et al. Light at night increases body mass by shifting the time of food intake. Proc. Natl. Acad. Sci. USA. 2010; 107:18664–18669. [PubMed: 20937863]
46. Scheer FA, Hilton MF, Mantzoros CS, Shea SA. Adverse metabolic and cardiovascular consequences of circadian misalignment. Proc. Natl. Acad. Sci. USA. 2009; 106:4453–4458. [PubMed: 19255424]
47. Reyes TM, Walker JR, DeCino C, Hogenesch JB, Sawchenko PE. Categorically distinct acute stressors elicit dissimilar transcriptional profiles in the paraventricular nucleus of the hypothalamus. J. Neurosci. 2003; 23:5607–5616. [PubMed: 12843263]
48. Roberts LD, et al. Increased hepatic oxidative metabolism distinguishes the action of peroxisome proliferator-activated receptor δ from peroxisome proliferator-activated receptor γ in the ob/ob mouse. Genome Med. 2009; 1:115. [PubMed: 19968882]
49. Irizarry RA, et al. Summaries of Affymetrix GeneChip probe level data. Nucleic Acids Res. 2003; 31:e15. [PubMed: 12582260]
50. Grant GR, Liu J, Stoeckert CJ Jr. A practical false discovery rate approach to identifying patterns of differential expression in microarray data. Bioinformatics. 2005; 21:2684–2690. [PubMed: 15797908]

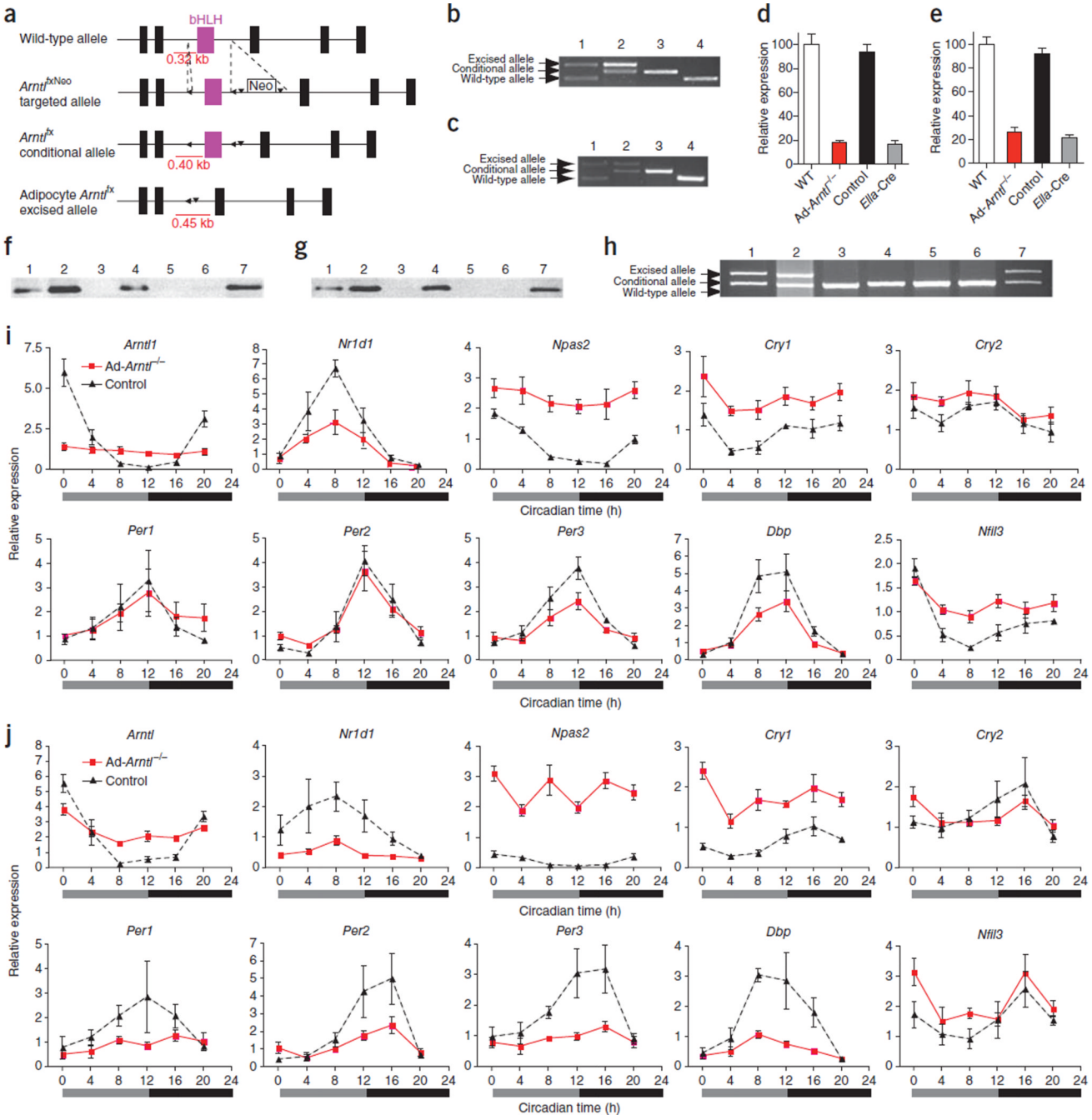

Figure 1.

Adipocyte-specific deletion of *Arntl* disrupts molecular rhythms in clock and clock-output gene expression. (a) Schematic diagram illustrating the region surrounding the basic helix-loop-helix (bHLH, purple) domain of the mouse *Arntl* locus, the targeted *Arntl*^{fxNeo} allele, the conditional *Arntl*^{fx} allele and the *Arntl*^{fx}-excised allele. (b,c) PCR products amplified from adipocyte genomic DNA isolated from epididymal WAT (b) and interscapular BAT (c). 1, ubiquitous *Ella*-Cre$^{+/-}$ *Arntl*$^{fx/+}$; 2, *aP2*-Cre$^{+/-}$ *Arntl*$^{fx/fx}$; 3, *Arntl*$^{fx/fx}$, no Cre; 4, *Arntl*$^{+/+}$, no Cre. (d,e) mRNA levels of *Arntl* quantified in primary adipocytes isolated from epididymal WAT (d) or interscapular BAT (e) from WT, *aP2*-Cre$^{+/-}$ *Arntl*$^{fx/fx}$ (Ad-*Arntl*$^{-/-}$), *Arntl*$^{fx/fx}$, no Cre (control) or ubiquitous *Ella*-Cre$^{+/-}$ *Arntl*$^{fx/fx}$ (*Ella*-Cre) mice. Error bars,

s.e.m. (f,g) Western blot analysis of Arntl in white (f) and brown (g) adipocytes. 1, *aP2*-Cre *Arntl*$^{+/+}$; 2, *Arntl*$^{fx/fx}$, no Cre; 3, *aP2*-Cre$^{+/-}$ *Arntl*$^{fx/fx}$; 4, *Arntl*$^{+/+}$, no Cre; 5, *Arntl*$^{-/-}$; 6, negative control; 7, positive control. (h) PCR products amplified from genomic DNA isolated from different tissues of *aP2*-Cre$^{+/-}$ *Arntl*$^{fx/fx}$ mice. 1, WAT; 2, BAT; 3, liver; 4, skeletal muscle; 5, hypothalamus; 6, adrenals; 7, peritoneal macrophages. (i,j) Clock and clock-controlled gene expression in epididymal WAT (i) and subscapular BAT (j) from adipocyte-specific *Arntl* knockout mice (Ad-*Arntl*$^{-/-}$) with *ad libitum* access to food (20-week-old mice on a regular diet; $n = 4$ for each time point and group). Relative expressions are normalized to *Gapdh* and plotted in arbitrary linear units (mean ± s.e.m.).

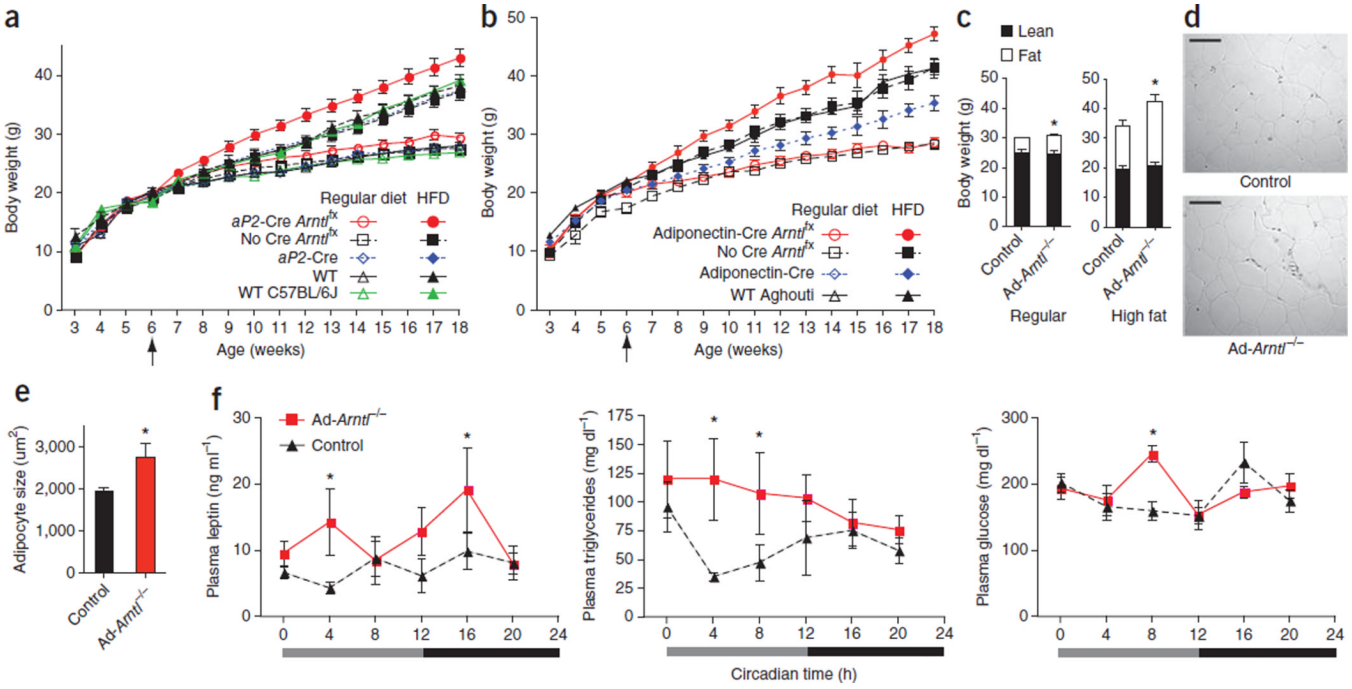

Figure 2.

Obesity in adipocyte-specific *Arntl* knockout (Ad-*Arntl*$^{-/-}$) mice. (a) Body weights of adipocyte-specific *Arntl* knockout mice (*aP2*-Cre *Arntl*^{fx}), littermate *Arntl*^{fx} controls (No Cre *Arntl*^{fx}), *aP2*-Cre controls (*aP2*-Cre), WT littermates of *aP2*-Cre controls (WT) and WT mice (WT C57BL/6J) ($n = 12$ per group). (b) Body weights of adipocyte-specific *Arntl* knockout mice (adiponectin-Cre *Arntl*^{fx}), littermate *Arntl*^{fx} controls (No Cre *Arntl*^{fx}), adiponectin-Cre controls (adiponectin-Cre) and WT littermates of adiponectin-Cre controls (WT Aghouti) fed either regular chow (open symbols) ($n = 6$) or HFD starting at 6 weeks of age ($n = 9$). (c) Body composition of 32-week-old Ad-*Arntl*$^{-/-}$ and control mice fed a regular diet, and 16-week-old Ad-*Arntl*$^{-/-}$ and control mice fed HFD ($n = 5$ per group). *$P <$ 0.05 by two-sample parametric *t* test. (d) Representative H&E stain images of epididymal WAT tissue isolated from 20-week-old weight-matched Ad-*Arntl*$^{-/-}$ and control mice on regular diet. Scale bars, 100 μm. (e) Adipocyte area size quantification for white adipocytes from epididymal WAT from weight-matched Ad-*Arntl*$^{-/-}$ and control mice (20-week-old mice fed a regular diet). *$P < 0.05$ by two-sample parametric *t* test. (f) Plasma concentrations of leptin, triglycerides and glucose at different time points of circadian time in 20-week-old mice kept under constant darkness with *ad libitum* access to a regular chow diet ($n = 4$ for each time point and group). *$P < 0.05$ by two-sample Mann-Whitney test. All data in the figure are the mean ± s.e.m.

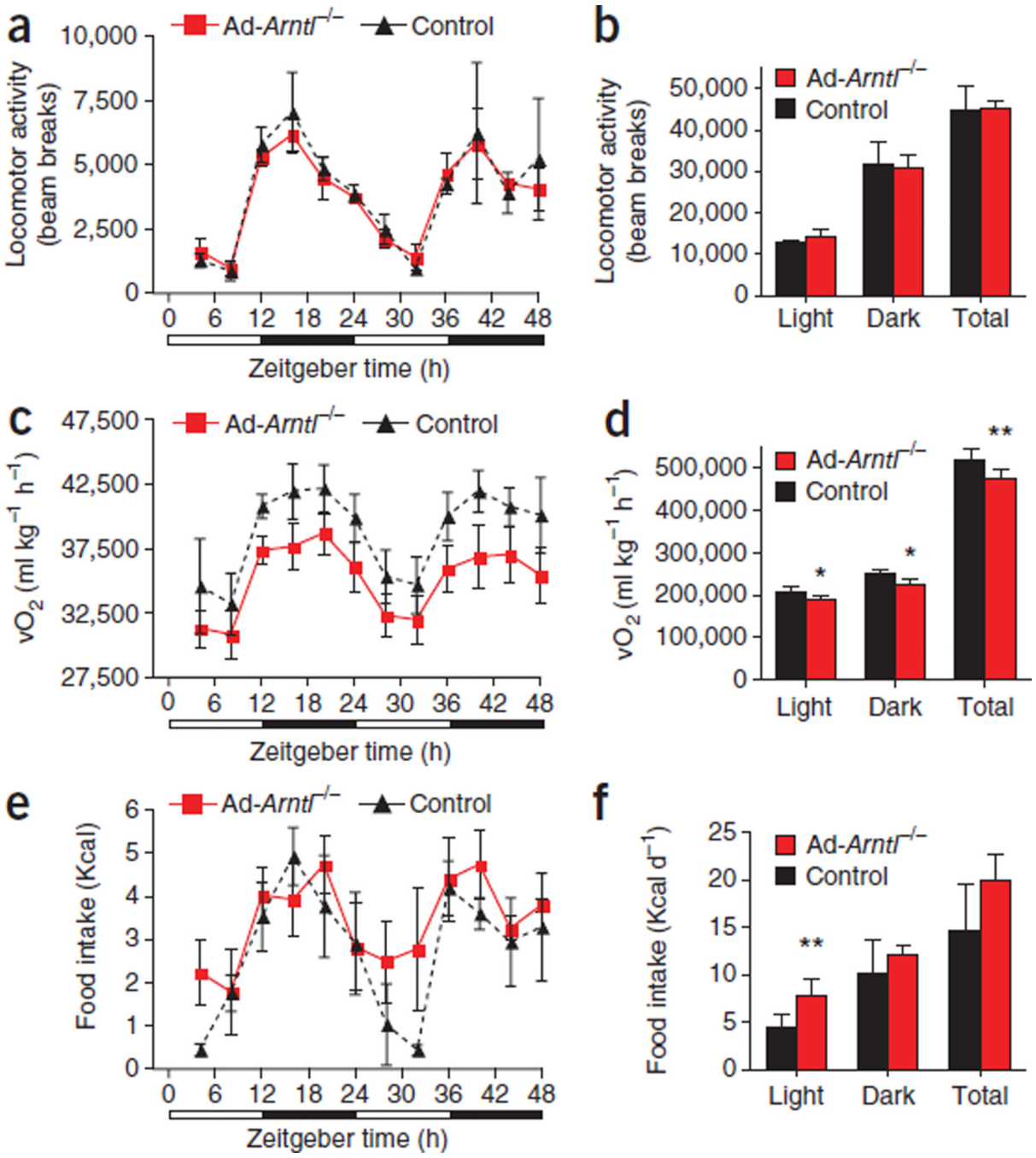

Figure 3.

Attenuation of the diurnal rhythm in feeding activity and lower energy expenditure in adipocyte-specific *Arntl* knockout mice (Ad-*Arntl*$^{-/-}$). (a–f) Locomotor activity (a,b), O_2 consumption rate (vO_2) (c,d) and food intake (e,f) monitored over two consecutive 24-h cycles for 20-week-old mice kept in 12-h light, 12-h dark conditions and fed HFD for 1 week. Results are represented as the totals for the light and dark periods in b, d and f ($n = 8$ per group). *$P < 0.05$, **$P < 0.01$ by two-sample Mann-Whitney test. vO_2 values are corrected for body weight, and correction for lean body mass produced similar results. All data in the figure are the mean ± s.e.m.

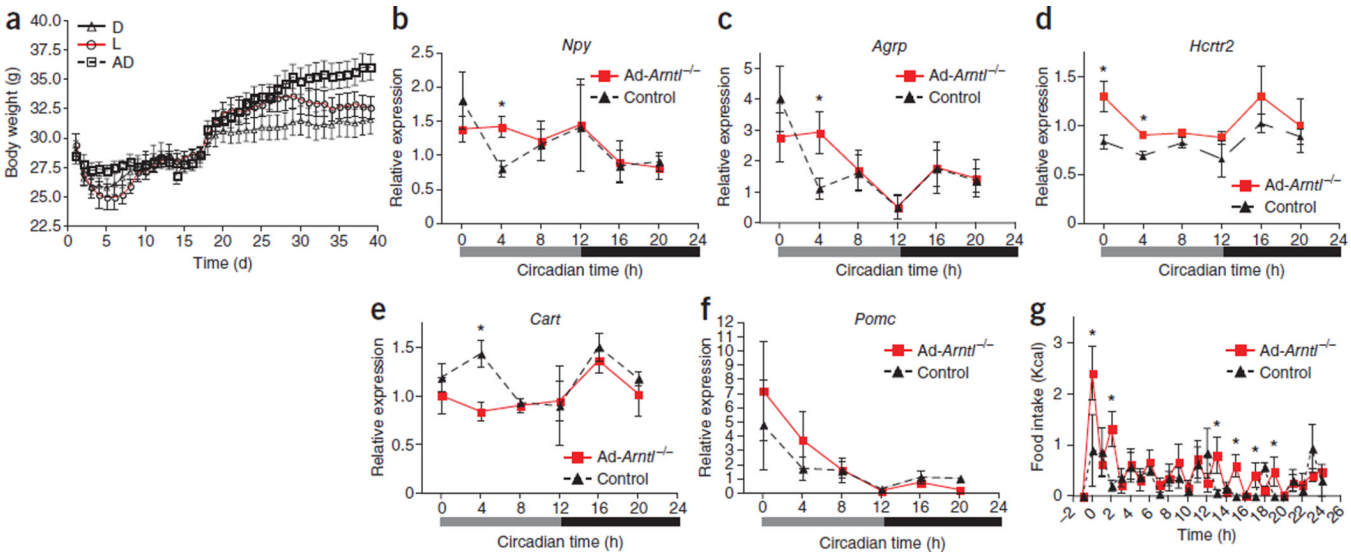

Figure 4.

Higher food intake during the light period leads to obesity. (a) Body weight in adipocyte-specific 20-week-old *Arntl* knockout mice (Ad-*Arntl*$^{-/-}$) fed the same amount of daily calories with access to food (i) only during the light period (L), (ii) only during the dark period (D) or (iii) *ad libitum* (AD) (n = 6 per group). Mice required an adjustment period to the feeding regimen, after which they were introduced to HFD (day 17). Body weight was monitored twice daily at the beginning of the light and dark phases. Results are the average of the two measurements (mean ± s.e.m.). (b–f) Time-specific alterations in hypothalamic expression of appetite-regulating neuropeptides. mRNA levels are quantified in hypothalamic sections isolated from regular diet–fed 20-week-old mice kept in constant darkness and fasted for 24 h before tissue collection (n = 4 for each time point and group). Relative expressions are normalized to *Gapdh* and plotted in arbitrary linear units (mean ± s.e.m.). *P < 0.05 by two-sample Mann-Whitney test. Results are representative of three independent experiments. (g) Food intake in response to a fasting and re-feeding challenge monitored over 24 h for mice kept in 12-h light, 12-h dark conditions. Refeeding started at time 0 after a 24-h fast (n = 8 20-week-old mice fed regular diet per group). *P < 0.05 by two-sample Mann-Whitney test.

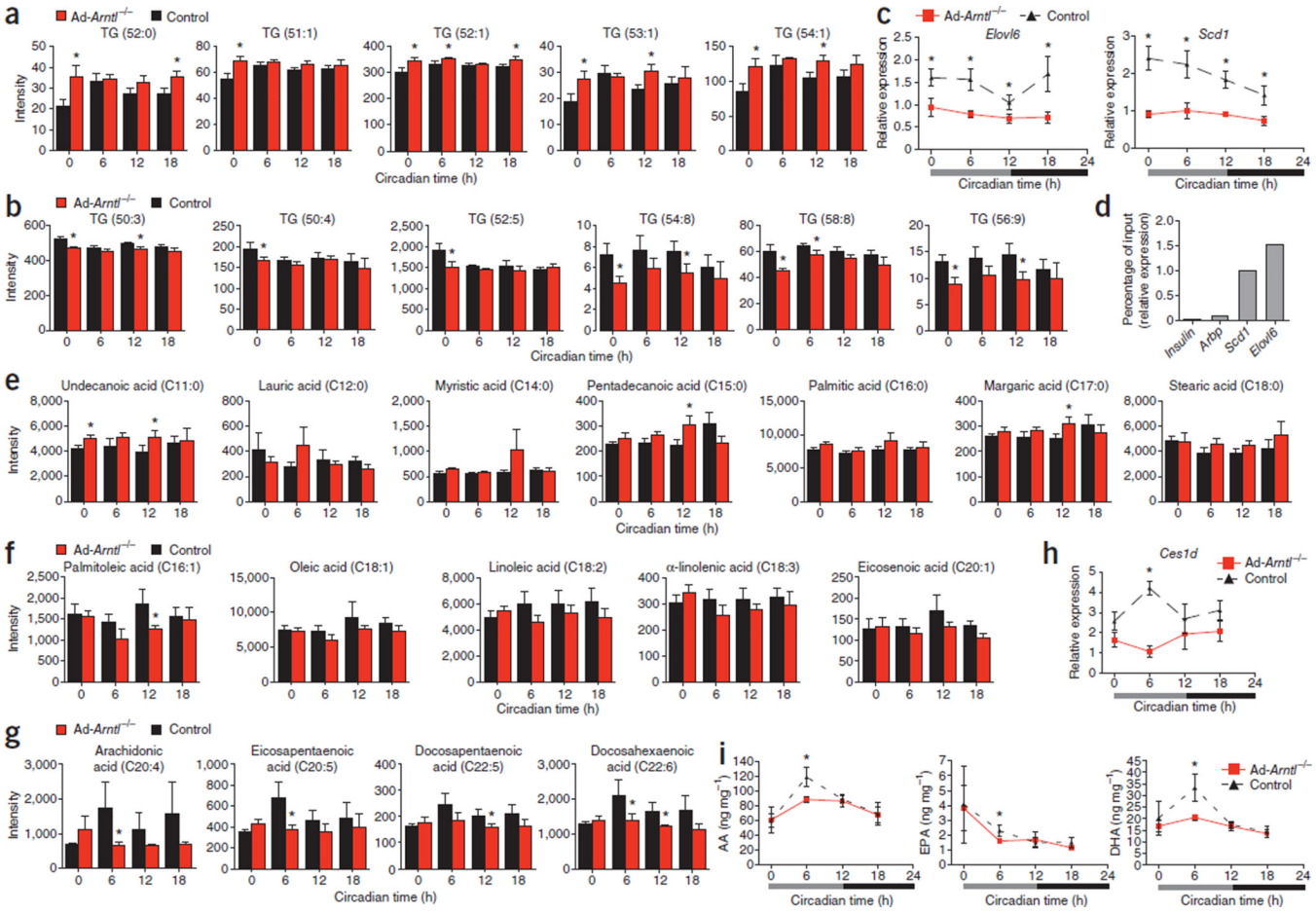

Figure 5.

Lower concentrations of polyunsaturated fatty acids in adipose tissue, plasma and hypothalamus of adipocyte-specific *Arntl* knockout mice (Ad-*Arntl*$^{-/-}$). (a,b) Relative concentration of triglycerides in WAT from regular diet–fed mice. (c) mRNA levels in WAT isolated from regular diet–fed mice. (d) Binding of Arntl to the promoters of *Elovl6* and *Scd1* as determined in epididymal adipose tissue by ChIP at zeitgeber time 10 (ZT10). Quantitative PCR–determined binding of DNA fragments of the *Elovl6* and *Scd1* promoters to Arntl expressed as a percentage of the detection of the same fragments in the input DNA used for ChIP. Regions close to the transcriptional starting site of the insulin and *Arbp* genes served as negative controls. (e–g) Amounts of fatty acids in plasma from regular diet–fed mice. (h) mRNA levels in WAT isolated from regular diet–fed mice. (i) Hypothalamic amounts of arachidonic acid (AA), EPA and DHA in regular diet–fed mice. In all experiments, data are expressed as the mean ± s.e.m. Relative expression mRNA levels are normalized to *Gapdh* and plotted in arbitrary linear units. For a–c and e–i, experiments were performed on regular diet–fed 20-week-old mice kept in constant darkness and fasted for 24 h before tissue collection (n = 6 for each time point and group).

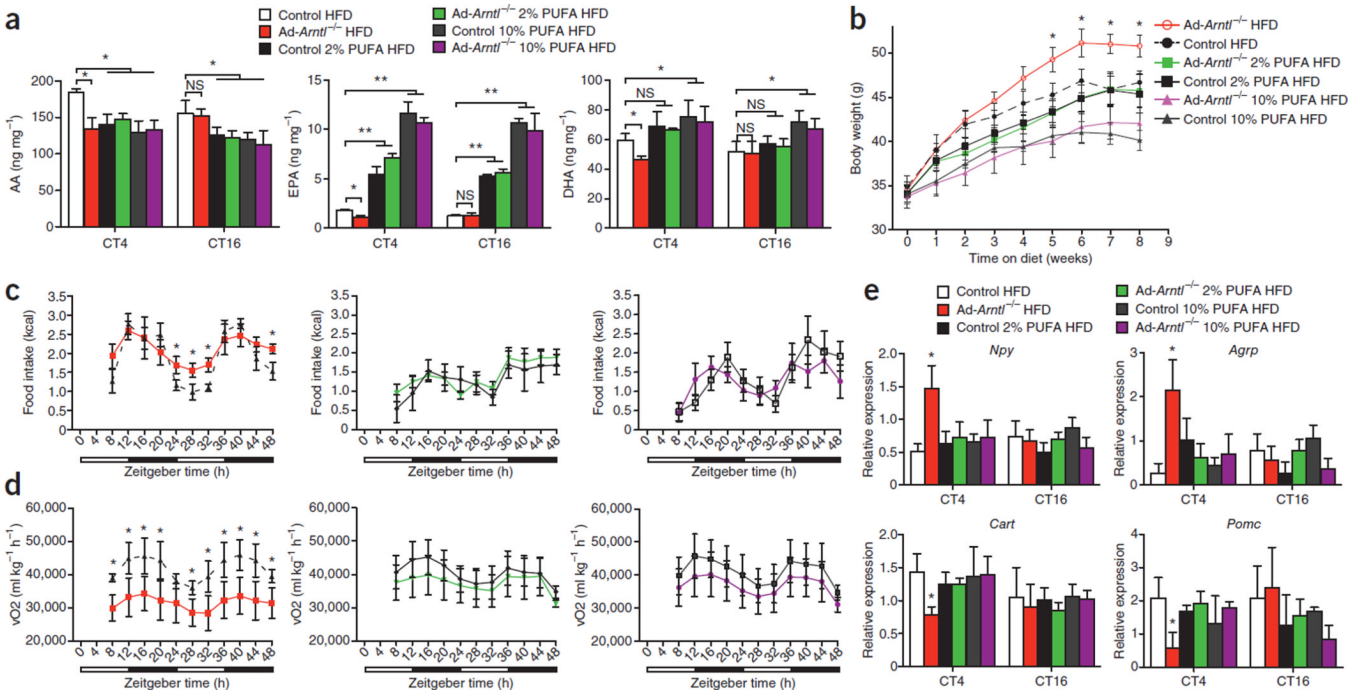

Figure 6.

Polyunsaturated fatty acid–rich diets restore hypothalamic polyunsaturated fatty acid content and correct body weight, feeding behavior, energy homeostasis and hypothalamic neuropeptide expression in adipocyte-specific *Arntl* knockout mice (Ad-*Arntl*$^{-/-}$). (a) Hypothalamic amounts of nonesterified arachidonic acid (AA), EPA and DHA after 8 weeks on the indicated diet at CT4 and CT16 of 30-week-old Ad-*Arntl*$^{-/-}$ and control mice kept in constant darkness and fasted for 24 h before tissue collection. HFD, high-fat diet providing 43% of the total energy from fat; 2% PUFA HFD, diet providing 2% of the total energy from EPA (1.2%) and DHA (0.8%) and 43% from fat; 10% PUFA HFD, diet providing 10% of the total energy from EPA (6%) and DHA (4%) and 43% from fat; PUFA, polyunsaturated fatty acid. $n = 6$ for each group and diet throughout. (b) Body weights of Ad-*Arntl*$^{-/-}$ and control mice during the 8 weeks on the three diets. (c,d) Food intake (c) and vO_2 (d) monitored over two consecutive 24-h cycles of mice on the three diets kept in 12-h light, 12-h dark conditions. (e) Hypothalamic expression of appetite-regulating neuropeptides after 8 weeks on the diet at CT4 and CT16. mRNA levels were quantified in hypothalamic sections isolated from mice kept in constant darkness and fasted for 24 h before tissue collection. Relative expressions are normalized to *Gapdh* and plotted in arbitrary linear units. All data in the figure are the mean ± s.e.m. NS, not significant, $*P < 0.05$, $**P < 0.01$ by two-sample Mann-Whitney test.